TIC 308396022: δ Scuti-γ Doradus hybrid with large-amplitude radial fundamental mode and regular g-mode period spacing

Tao-Zhi Yang, Zhao-Yu Zuo, Gang Li, Timothy R. Bedding, Simon J. Murphy, Meridith Joyce

A&A 655, A63 (2021)
https://doi.org/10.1051/0004-6361/202142198

Astronomy & Astrophysics

TIC 308396022: δ Scuti–γ Doradus hybrid with large-amplitude radial fundamental mode and regular *g*-mode period spacing

Tao-Zhi Yang[1], Zhao-Yu Zuo[1], Gang Li[2], Timothy R. Bedding[3,4], Simon J. Murphy[3,4], and Meridith Joyce[5]

[1] Ministry of Education Key Laboratory for Nonequilibrium Synthesis and Modulation of Condensed Matter, School of Physics, Xi'an Jiaotong University, 710049 Xi'an, PR China
e-mail: zuozyu@xjtu.edu.cn
[2] IRAP, Université de Toulouse, CNRS, CNES, UPS, Toulouse, France
[3] Sydney Institute for Astronomy (SIfA), School of Physics, University of Sydney, Camperdown, NSW 2006, Australia
[4] Stellar Astrophysics Centre, Department of Physics and Astronomy, Aarhus University, Ny Munkegade 120, 8000 Aarhus C, Denmark
[5] Space Telescope Science Institute in Baltimore, Baltimore, MD, USA

Received 10 September 2021 / Accepted 30 September 2021

ABSTRACT

We analyse the pulsating behaviour of TIC 308396022, based on observations by the TESS mission. The star is a high-amplitude δ Sct star that shows a very rich amplitude spectrum using the 3-yr light curve. Among these frequencies, the strongest peak of $f_1 = 13.20362567(12)\,\mathrm{d}^{-1}$ is identified as the radial fundamental mode, and we also find the first and second overtones (f_2 and f_3). In the low-frequency range (<2.5 d^{-1}), 22 peaks are identified as gravity modes, which show a regular period spacing of about 2460 s and have an angular degree of $l = 1$. The period spacing pattern does not show a significant downward trend, suggesting the star is rotating slowly. We note that this is a δ Sct–γ Dor hybrid star containing a high-amplitude radial fundamental mode and a regular *g*-mode period spacing pattern. With the $O-C$ analysis, we find the star shows a significant time delay, implying that the star has a companion and it is likely to be a white dwarf. The history of possible mass transfer provides a great opportunity for testing the current theories of binary evolution, mass transfer, and pulsation.

Key words. stars: oscillations – stars: variables: δ Scuti – stars: individual: TIC 308396022

1. Introduction

The study of stellar oscillations is a powerful tool for probing the internal structures of stars by using stellar periodic oscillations (Aerts et al. 2010; Chaplin & Miglio 2013; Catelan & Smith 2015; Aerts 2021). Oscillations can be observed photometrically (Handler 2013; Aerts 2021) and pulsation frequencies can be found by calculating the amplitude spectrum (e.g. Lomb 1976; Scargle 1982). Subsequently, many parameters such as mass, age, rotation, and distance can be measured, which is valuable as observing them is not otherwise straightforward.

A certain class of short-period pulsating stars, δ Sct stars, shows great potential for asteroseismic studies. They are intermediate-mass variables with spectral types between A2 and F2, and situated in the lower end of the classical instability strip (Breger 2000; Murphy et al. 2019). Most δ Sct stars are multi-periodic pulsators and may show radial and non-radial pulsations (Bowman 2017). These pulsations are driven by the κ mechanism operating in the He-II partial ionisation zone (Breger 2000; Aerts et al. 2010; Antoci et al. 2014; Murphy et al. 2020); therefore, the pulsations are low-radial-order (n), low-angular-degree (l) pressure (p) modes with periods between 15 min and 8 h (Uytterhoeven et al. 2011; Holdsworth et al. 2014). Their masses are generally between 1.5 $M_\odot$ and 2.5 $M_\odot$, which place them in the transition region, the lower mass stars with a thick outer convective envelope and the massive cases with thin convective shell (Bowman 2017). Thus, the pulsations in δ Sct stars provide an opportunity to carry out detailed studies for the structure and evolution of stars in this transition region (Bowman & Kurtz 2018).

However, the amplitude spectra of δ Sct stars are generally very rich and messy, which challenges the mode identification (Goupil et al. 2005; Handler 2009a). Recently, Bedding et al. (2020) found that some young multi-periodic δ Sct stars show regular frequency separations as predicted by the asymptotic relation (Shibahashi 1979; Tassoul 1980), providing a new possibility for asteroseismology in δ Sct stars. In addition, there is a sub-class δ Sct stars named high-amplitude δ Sct stars (HADS), whose mode identification is relatively clear. The HADS usually pulsate in the radial fundamental mode and overtones, with amplitudes of about 0.1 magnitude (Petersen 1989; Petersen & Christensen-Dalsgaard 1996). The target in this work, TIC 308396022, is a HADS.

Furthermore, A- to F-type main-sequence (MS) stars may also pulsate in gravity (g) modes. These are known as γ Dor stars, which appear near the red edge of the δ Sct instability strip and show low-frequency light variations (Balona et al. 1994; Kaye et al. 1999; Dupret et al. 2005a). These stars have typical masses from 1.4 to 2.0 $M_\odot$ (e.g. Kaye et al. 1999; Van Reeth et al. 2016) and they usually pulsate in low-degree high-order g modes driven by the convective blocking mechanism (Guzik et al. 2000; Dupret et al. 2004, 2005a), with periods between 0.2 days and 2 days and typical amplitudes below 0.01 mag (Li et al. 2020). The g modes sometimes show uniform spacings in period, as predicted by the asymptotic relation. Usually, the uniform period spacings contain the information of

the inner chemical composition gradients and the stellar evolutionary status (e.g. Miglio et al. 2008; Wu et al. 2018, 2020; Moravveji et al. 2015; Wu & Li 2019; Sekaran et al. 2021). However, for some special case, they also contain other information, such as near-core rotation rates (Bouabid et al. 2013; Ouazzani et al. 2017) and coupling between g modes and inertial modes (Ouazzani et al. 2020; Saio et al. 2021).

The overlapping of the instability strips of δ Sct and γ Dor stars supports the existence of hybrid stars that show both p- and g-mode pulsations (Breger & Beichbuchner 1996). The g modes carry the information of the near-core region and the p modes can probe the stellar envelope (Grigahcène et al. 2010; Kurtz et al. 2014; Saio et al. 2015), so the hybrid pulsators of δ Sct and γ Dor stars have a great potential to contribute to our understanding of the internal structure of a star (see Kurtz et al. 2014; Saio et al. 2015; Schmid & Aerts 2016; Sánchez Arias et al. 2017). Several δ Sct–γ Dor hybrid stars have been detected by ground-based observations (Handler & Shobbrook 2002; Henry & Fekel 2005; Handler 2009b) and the large number observed by space missions such as CoRoT (Baglin et al. 2009) and *Kepler* (Borucki et al. 2010) suggest that hybrid behaviour might be common among A-F stars (Grigahcène et al. 2010; Hareter et al. 2010). Based on a large sample (750 stars) of δ Sct and γ Dor candidates discovered in *Kepler* mission, Uytterhoeven et al. (2011) found that about 63% (471 stars) of the sample show δ Sct or γ Dor pulsations, and 36% (171 stars) are hybrid δ Sct–γ Dor stars. Recent studies (e.g. Bradley et al. 2015) with a larger sample of δ Sct–γ Dor stars suggest that hybrid stars are very common. With the successful launch of TESS mission (Ricker et al. 2014, 2015), more hybrid stars will be found and hence provide better understandings for the inner structures and oscillation spectra of this kind of variables.

TIC 308396022 (TYC 8928-1300-1; $\alpha_{2000} = 08^{\rm h}01^{\rm m}02\overset{\rm s}{.}370$, $\delta_{2000} = -63°40'30\overset{''}{.}317$) was first observed in Sector 1 of the TESS observations and classified as a pulsating star in Antoci et al. (2019). Its basic properties from that study and the TESS Input Catalogue (TIC; Stassun et al. 2018) are listed in Table 1. To investigate the pulsations of TIC 308396022 further, we analyse the 2-min cadence photometric data spanning three years from the TESS mission.

Table 1. Basic parameters of TIC 308396022.

Parameters	TIC 308396022	References
TESS magnitude	11.069	a
Alternative ID	GSC 08928–01300	a
	2MASS J08010239–6340302	
$T_{\rm eff}$	6730 ± 248 K	(*Gaia*), a
	6860 ± 150 K	SED, b
	7371 ± 150 K	SED, c
log g	3.81 ± 0.25 dex	(*Gaia*, phot), a
	4.12 ± 0.25 dex	c
log $(L/L_\odot)$	0.94 ± 0.01	(*Gaia*), a
Parallax (mas)	1.71 ± 0.02	(*Gaia*), a
B	11.55	c
V	10.997	c
J	10.573	c
H	10.471	c
K	10.371	c
Gaia mag	11.330	a

References. (*a*) *Gaia* (McDonald et al. 2017). (*b*) Antoci et al. (2019). (*c*) Parameters from the TESS Input Catalogue (Stassun et al. 2018): https://tasoc.dk/catalog/.

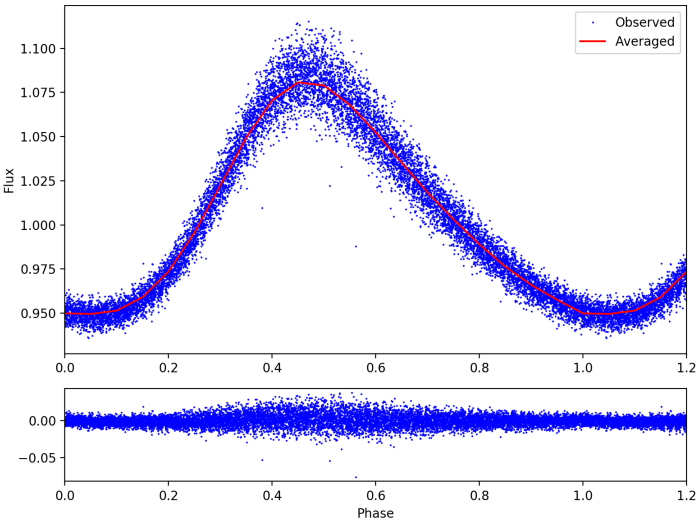

Fig. 1. Phase diagram of TIC 308396022 from TESS data, folded by the frequency, $f_1 = 13.20362567\,{\rm d}^{-1}$. The obvious light variation of rapid climb and slow descent is typical for a HADS star.

2. Observation and data reduction

TIC 308396022 was observed in Sectors 1, 4, 5, and 7–11 during the first cycle of the TESS mission, and again in Sectors 27, 28, 31, 34, 35, 37, and 38 during Cycle 3. We use all these light curves, which are available from the Mikulski Archive for Space Telescopes (MAST)[1]. We downloaded all the data and used the 2-min cadence Simple Aperture Photometry (SAP) light curves for our research. In each sector, the obvious outliers were removed and the slow trend was corrected with a high-pass filter. In total, the rectified light curve includes 236991 data points spanning 1035 days with a duty-cycle of 32%. Figure 1 shows the phased light curve, folded by the dominant frequency $f_1 = 13.20362567(12)\,{\rm d}^{-1}$. The peak-to-peak amplitude of the dominant mode is ~14.7%.

3. Frequency analysis and mode identification

To extract the pulsation frequencies, we calculated the Fourier transform of the reduced light curve using the software PERIOD04 (Lenz & Breger 2005). The peaks are extracted one-by-one via the method of pre-whitening, in the processes, the light curve is fitted with the following formula:

$$m = m_0 + \Sigma A_i \sin(2\pi(f_i t + \phi_i)), \quad (1)$$

where m_0 is the zero-point, A_i, f_i, and ϕ_i are the amplitude, frequency, and phase, respectively, of the ith peak.

We extracted all the frequencies with $S/N > 4.0$ (Breger et al. 1993) and $f < 80\,{\rm d}^{-1}$, which covers the typical pulsation frequency range of δ Sct stars. The uncertainties of frequencies were calculated following Montgomery & O'Donoghue (1999) and Kjeldsen & Bedding (2012):

$$\sigma_{\rm f} = 0.44 \frac{1}{T} \frac{1}{S/N}, \quad (2)$$

[1] MAST: http://archive.stsci.edu/

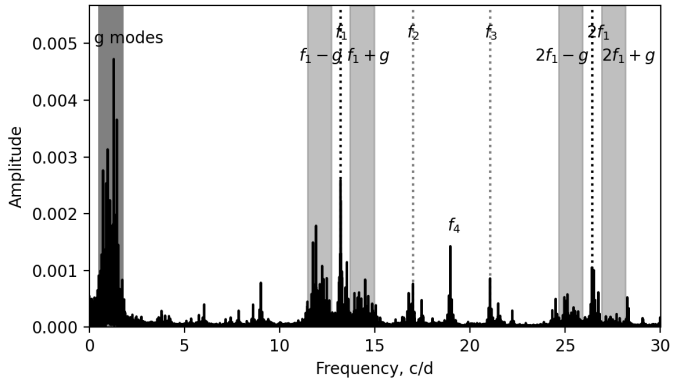

Fig. 2. Amplitude spectrum of TIC 308396022, with the fundamental mode removed. The vertical dark-gray dotted line marks the location of the fundamental mode f_1, and the light-gray dotted lines mark the first and the second overtones, f_2 and f_3. The dark shaded area shows the g-mode region, while the light shaded areas around f_1 and $2f_1$ show the combinations between the fundamental mode and the g modes: $f_1 + g$, $f_1 - g$, $2f_1 + g$, and $2f_1 - g$.

where $T = 1035$ d is the observation time span, and S/N is the signal-to-noise ratio of the peak. The noise is the mean level within 2.5 c/d around the peak.

3.1. Pressure modes

Based on the *Gaia* EDR3 distance of 591 ± 11 pc (Bailer-Jones et al. 2021) and the apparent magnitude of $V = 11.0$, we calculated the absolute magnitude to be $M_V = 2.14 \pm 0.04$ (neglecting extinction). According to the period-luminosity relation from Ziaali et al. (2019), the frequency of the radial fundamental mode is expected to be about $13.86 \pm 0.43\,\mathrm{d}^{-1}$. The dominant frequency of $f_1 = 13.20362567(12)\,\mathrm{d}^{-1}$ is therefore consistent with the radial fundamental, especially given the intrinsic scatter in the P–L relation. In fact, if we consider a small extinction ($A_V = 0.05$) for calculating the absolute magnitude M_V, then the P–L relation predicts the radial fundamental mode to be $13.3 \pm 0.4\,\mathrm{d}^{-1}$, in agreement with the observed mode.

The radial fundamental mode contributes the majority of the light variations. To see more details in the power spectrum, we removed the fundamental mode by the mean phased light curve shown in Fig. 1. In Fig. 2, we display the amplitude spectrum of the residuals. We still can see the residual of the strongest fundamental mode with a frequency of $f_1 = 13.20362567(12)\,\mathrm{d}^{-1}$. As discussed in Sect. 5, these are sidelobes split by the orbital frequency (Shibahashi & Kurtz 2012; Shibahashi et al. 2015). We note that a peak appears at $f_2 = 17.003479(8)\,\mathrm{d}^{-1}$, with a ratio of $f_1/f_2 = 0.7765$. Therefore, we identified the mode at f_2 as the first overtone. The second overtone is also found at $f_3 = 21.052996(7)\,\mathrm{d}^{-1}$ with a ratio of $f_1/f_3 = 0.6272$ (Stellingwerf 1979; Netzel et al. 2021). The p-mode frequencies and mode identifications are listed in Table 2. When assigning the radial orders, we followed the convention advocated by Gough (2000), namely, the fundamental mode is $n = 1$, the first overtone is $n = 2$, and the second overtone is $n = 3$.

Another stronger peak f_4 ($=18.96664\,\mathrm{d}^{-1}$) has a ratio of $f_1/f_4 = 0.696$, which is not equal to any value of the period ratios of the first four radial mode for δ Sct stars. Therefore, f_4 must belong to a non-radial mode. Given that f_4 is very close (within 0.33%) to halfway between f_2 (the first radial overtone) and f_3 (the second radial overtone), it is likely to be $l = 1$.

Table 2. Frequencies and identifications of the p modes in TIC 308396022.

Name	Frequency, d^{-1}	Radial order (n)	Angular degree (l)
f_1	13.20362567(12)	1	0
f_2	17.003479(8)	2	0
f_3	21.052996(7)	3	0
f_4	18.96664(1)	–	1

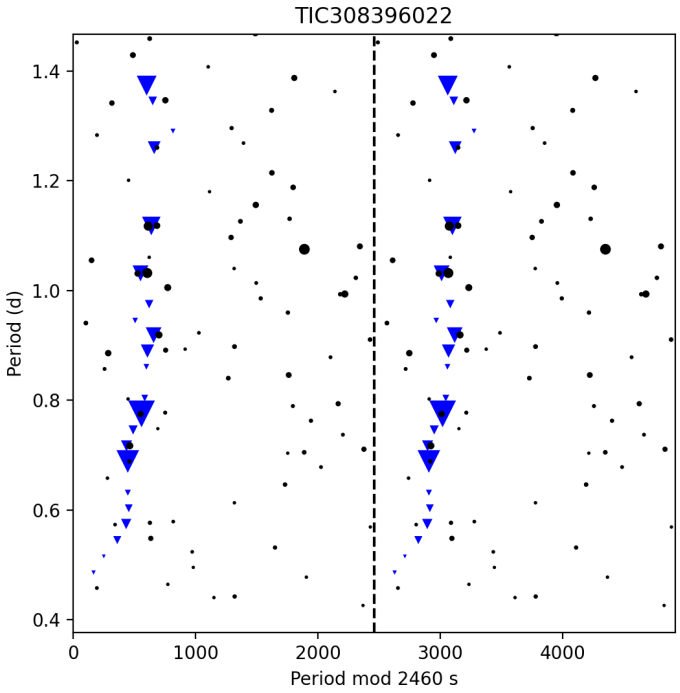

Fig. 3. Period échelle diagram of TIC 308396022, showing a clear period spacing of about 2460 s. The blue triangles indicate g modes with $l = 1$, while the black dots are probably noise peaks.

3.2. Gravity modes

The modes with frequencies below $\sim 2.5\,\mathrm{d}^{-1}$, shown as the dark shaded area in Fig. 2, are below the typical frequency range of δ Sct stars. We also see the combinations between the fundamental mode f_1 and these low frequencies, marked by the light shaded areas in Fig. 2, which proves that they originate from the same star.

To identify these modes, we made the period échelle diagram for TIC 308396022, following the method described in Bedding et al. (2015) and Li et al. (2019a). The result is shown in Fig. 3 and Table 3. It clearly shows the properties of the uniform period spacing with a period spacing ΔP of about 2460 s, which is within the typical range for dipole $l = 1$ g modes in γ Dor stars (Van Reeth et al. 2015, 2016; Li et al. 2019b). We show the period spacing pattern in Fig. 4, and find that the period spacings ΔP fluctuate around 2500 s, but do not show a clear downward trend. The obvious fluctuation implies that TIC 308396022 might be an evolved star and far from the zero-age main-sequence (ZAMS) (Miglio et al. 2008; Wu et al. 2018). Following the method by Van Reeth et al. (2016) and Li et al. (2019a), we obtain the asymptotic spacing as $\Pi_0 = \sqrt{l(l+1)}\Delta P = 3655 \pm 13$ s, which is smaller than the typical

Table 3. Frequencies and periods of the g modes.

Frequency, d^{-1}	Period, d	Radial order
2.05778(6)	0.485961(14)	17
1.94024(8)	0.515400(20)	18
1.834369(18)	0.545147(5)	19
1.740762(11)	0.574461(4)	20
1.657888(19)	0.603177(7)	21
1.58337(3)	0.631564(13)	22
1.4524286(23)	0.6885020(11)	24
1.394985(9)	0.716853(5)	25
1.340569(14)	0.745952(8)	26
1.2899600(16)	0.775218(10)	27
1.243789(25)	0.803995(16)	28
1.16131(4)	0.861095(26)	30
1.124017(7)	0.889666(5)	31
1.088470(5)	0.918721(4)	32
1.05770(4)	0.94545(3)	33
1.025381(16)	0.975247(15)	34
0.969583(5)	1.031371(5)	36
0.894606(3)	1.117810(4)	39
0.793373(7)	1.260441(11)	44
0.77478(5)	1.29069(8)	45
0.743097(15)	1.345720(28)	47
0.7280023(29)	1.373622(6)	48

Notes. The numbers in the brackets show the uncertainties in the last digits. The radial order is calculated by the period divided by the period spacing ΔP, which is set $\Delta P = 2460$ s.

value of the γ Dor stars (about 4000 s, see Li et al. 2020). The small asymptotic spacing value also shows that this star has evolved to the end of the MS. However, the flat period spacing pattern indicates that the near-core rotation is slow, so that the effect of the Coriolis force is negligible (Bouabid et al. 2013). Based on the method from Van Reeth et al. (2016) and Li et al. (2019a), we estimate the rotation rate as $0.006 \pm 0.003\,d^{-1}$. We note that the slope in the ΔP–P relation is very small and it is strongly influenced by the scatter rather than the rotation effect, hence, the rotation rate we give is imprecise. Slow rotation is also consistent with the assumption that the only difference between the HADS and small-amplitude δ Sct stars is the rotation rate (Xiong et al. 2016).

4. Location in the H-R Diagram

To investigate the evolutionary state of TIC 308396022, we calculated its luminosity as: $L = 9.31 \pm 0.50\,L_\odot$ ($\log L/L_\odot = 0.97 \pm 0.02$) using the parameters from TIC (Stassun et al. 2018). Based on the luminosity $\log L/L_\odot = 0.97 \pm 0.02$ and $T_{\rm eff} = 7371 \pm 150$ K from the TIC, we plot the location of TIC 308396022 in the H-R Diagram shown in Fig. 5, as well as additional 34 well-studied HADS stars collected from literature (McNamara 2000; Poretti et al. 2005, 2011; Christiansen et al. 2007; Balona et al. 2012; Ulusoy et al. 2013; Peña et al. 2016; Yang et al. 2018; Yang & Esamdin 2019). From this figure, we can see that TIC 308396022 lies between the δ Sct and the γ Dor instability strip on the MS. We note that both the effective temperatures derived from *Gaia* and Antoci et al. (2019) are lower than that from TIC, which sets TIC 308396022 far apart from the HADS region and δ Sct instability strip.

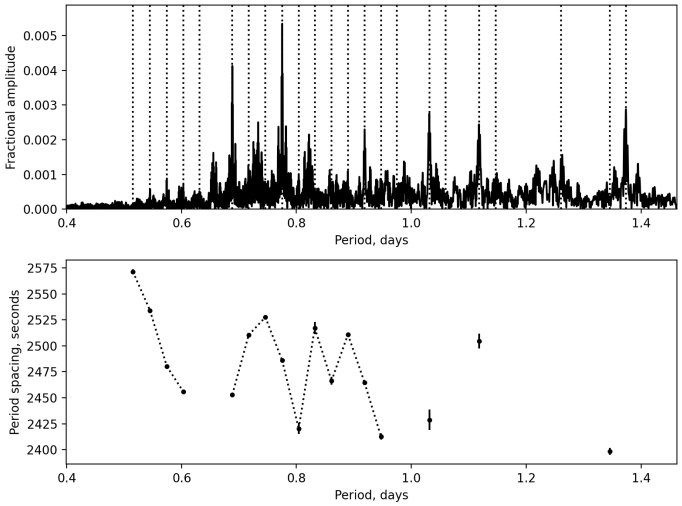

Fig. 4. Amplitude spectrum and period spacing patterns of TIC 308396022. *Upper panel*: amplitude spectrum with x-axis of period. The vertical dashed lines show the locations of the g modes in the period spacing patterns. *Lower panel*: period spacing pattern. The dots are the period spacings between the adjacent modes.

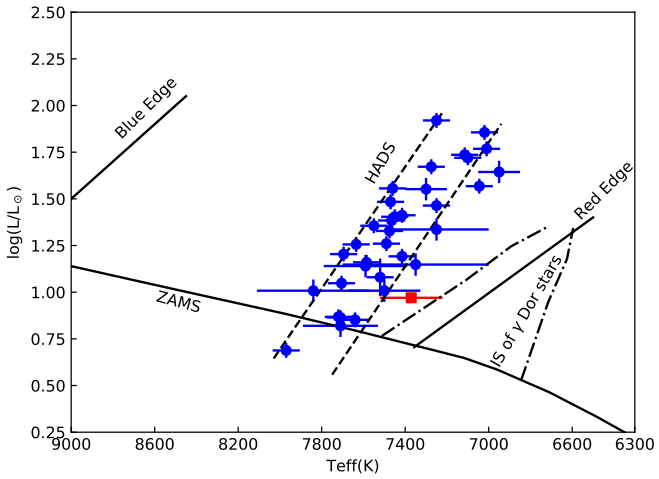

Fig. 5. Location of the 34 well-studied HADS and TIC 308396022 in the H-R Diagram. TIC 308396022 is shown as the red square. The blue dots are the HADS collected from McNamara (2000), Poretti et al. (2005, 2011), Christiansen et al. (2007), Balona et al. (2012), Ulusoy et al. (2013), Peña et al. (2016), Yang et al. (2018), Yang & Esamdin (2019), Bowman et al. (2021). The zero-age main-sequence (ZAMS) and the δ Sct instability strip (solid lines) are from Murphy et al. (2019). The dashed lines show the region occupied by HADS, as found by McNamara (2000). The theoretical instability strip (IS) of γ Dor stars (dotted-dashed lines) is from Dupret et al. (2005b).

5. Binary nature

By using the well-known 'Observed minus Calculated' (O–C) method (Sterken 2005), we measured the light maximum times of the fundamental mode and found a significant time shift, as shown in Fig. 6. The light maximum times vary from −200 s to about 100 s, and the maxima of the O–C diagram appear at about 1800 and 12 000 cycles, leading to a period of around 800 days. We deduce that the periodic variation of the light maximum time is caused by the orbital motion of the pulsating star TIC 308396022, as observed in many previous

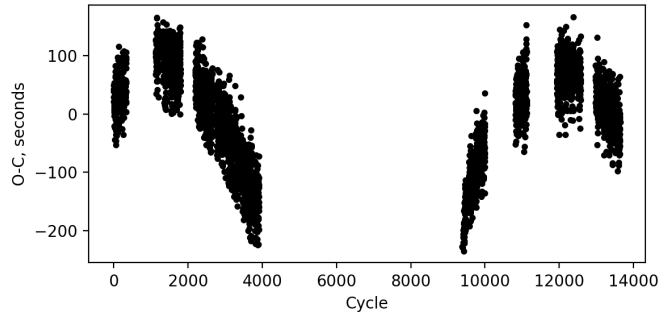

Fig. 6. $O-C$ diagram of TIC 308396022 based on the dominant pulsation mode (f_1).

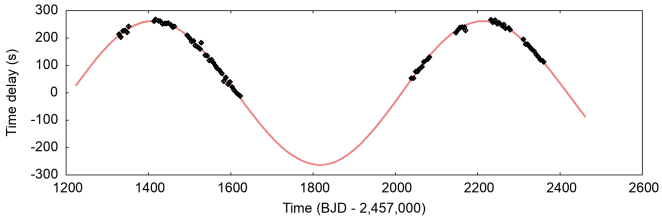

Fig. 7. Time delay measurements (black symbols) for TIC 308396022, using 10-d light curve segments. Overlapping red curves show 25 random samples from the Markov chain that are indistinguishable from this resolution.

large-amplitude variable stars (e.g. Fu & Sterken 2003; Conroy et al. 2014; Li et al. 2018).

To investigate the orbital parameters, we applied the phase-modulation method to the fundamental mode, f_1, and its harmonics, $2f_1$, $3f_1$, and $4f_1$ (Murphy et al. 2014, 2016; Murphy & Shibahashi 2015; Hey et al. 2020a,b), whose phase changes indicate that the light travel effect is due to the orbital motion, hence allowing us to determine the orbital parameters. Figure 7 displays the time delay and the best-fitting model. The medians and one-sigma uncertainties from the positions of a Monte Carlo Markov chain (MCMC) give an orbital period of 803.5 ± 0.6 d, projected semi-axis of $a_1 \sin i/c$ = 262.9 ± 1.2 s, eccentricity of e = 0.015 ± 0.006, and mass function of $f(M_1, M_2, \sin i) = \frac{(m_2 \sin i)^3}{(m_1+m_2)^2}$ = 0.0302 ± 0.0004 $M_\odot$. Assuming the mass of TIC 308396022 is 1.5 $M_\odot$ (2.5 $M_\odot$), the mass of the secondary is 0.49 $M_\odot$ (0.67 $M_\odot$) for the inclination i = 90°, or 0.58 $M_\odot$ (0.8 $M_\odot$) for i = 60°, which is within the typical mass range for a C/O WD (Althaus et al. 2010; Córsico et al. 2019).

To investigate the possible evolutionary history of this system, an evolutionary population synthesis simulation was carried out, using the code developed initially by Hurley et al. (2000, 2002) and recently updated by Zuo & Li (2014). To simulate this system (M_1 ~ 1.5–2.5 $M_\odot$; M_2 ~ 0.49–0.8 $M_\odot$; $P_{\rm orb}$ ~ 800 days), the progenitor was found to have these features: mass of primary as ~1.7–2.8 $M_\odot$, secondary as ~1.4–2.2 $M_\odot$, and the initial orbits as ~200–600 $R_\odot$. Taking a typical system as the example, we chose a primordial binary system with masses of 2.3 $M_\odot$ (the primary) and 1.81 $M_\odot$ (the secondary) in a 413 $R_\odot$ orbit. The primary evolves and first arrives at its asymptotic giant branch (AGB) stage (at 1011 Myr), the radius of the expanding AGB star exceeds its Roche lobe (RL) and it starts mass-transfer to its companion (Lauterborn 1970; Karakas et al. 2000; Toonen et al. 2014). The orbit is circularised during the mass transfer process and then the system leaves a post-AGB star, and in this case, a 0.57 $M_\odot$ C/O WD with a 1.96 $M_\odot$ (rejuvenated) MS star in a 504 $R_\odot$ orbit, which is in line with the orbital parameter of this system. We note WDs are often found in low-eccentricity systems, and for A/F stars that are the primaries of systems in the period range detectable by *Kepler* (100–1500 d), 21% of the companions are WDs (Murphy et al. 2018). After that, the rejuvenated secondary evolves to expand and fills its RL on the AGB (at 1709 Myr). Then the binary may enter into a common envelope (see Ivanova et al. 2013 for reviews), leaving a double WD if it survives.

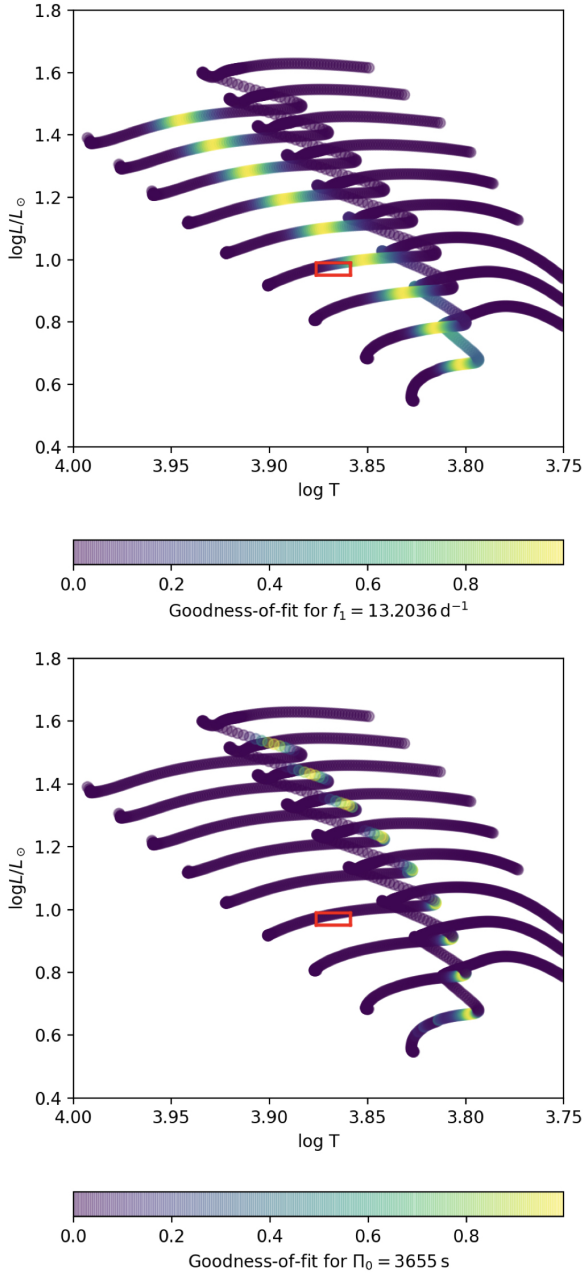

Fig. 8. Comparison between the observations and models with Z = 0.020, mixing length α = 2, and exponential overshooting $f_{\rm ov}$ = 0.02. The mass is between 1.4 and 2.2 solar masses, with steps of 0.1 solar masses. The red box shows the observed region ($T_{\rm eff}$ = 7371 ± 150 K, $\log L/L_\odot$ = 0.97 ± 0.02), and the color shows the goodness-of-fit for the fundamental mode (f_1, *top*) and asymptotic spacing (Π_0, *bottom*), which are proportional to $\exp[-(f_{1,\rm cal} - f_1)^2]$ and $\exp[-(\Pi_{0,\rm cal} - \Pi_0)^2]$, where $f_{1,\rm cal}$ and $\Pi_{0,\rm cal}$ are the model-derived fundamental mode and asymptotic spacing.

We calculated a coarse grid to construct a preliminary model of the pulsator under a single-star evolution, using the stellar evolution code MESA (v12778, Paxton et al. 2011, 2013, 2015, 2018, 2019) and the stellar oscillation code GYRE (e.g. Townsend & Teitler 2013). The parameters of the grid were: mass from 1.4 to 2.2 solar masses with step of 0.1 solar masses, metallicity $Z = 0.020$, mixing length $\alpha = 2$, and exponential overshooting $f_{\rm ov} = 0.02$. The results are shown in Fig. 8, where the colour represents the goodness-of-fit for the fundamental mode (f_1, top panel) and the g-mode asymptotic spacing (Π_0, bottom panel). We find that within the observation region ($T_{\rm eff} = 7371 \pm 150$ K, $\log L/L_\odot = 0.97 \pm 0.02$ derived in Sect. 4), there is no model that satisfies both the p- and g-mode pulsations. We also tried several other selections of metallicity ($Z = 0.0043, 0.0054, 0.0068, 0.0085, 0.010, 0.013, 0.016, 0.025$), but still could not find a compatible model. The absence of a compatible model implies that the star has different core and envelope formation histories, perhaps due to mass transfer from the secondary star. Some recent research has shown that asteroseismology has the ability to detect stellar merger or mass transfer in red giants (Rui & Fuller 2021; Deheuvels et al. 2021), and we suggest that TIC 308396022 might be a MS counterpart showing mass transfer by asteroseismology. We also note that Miszuda et al. (2021) performed binary-evolution and pulsational modellings of KIC 10661783, an δ Sct–γ Dor hybrid in an eclipsing binary system, and showed that a mass transfer has a significant impact on the g-mode excitations.

With the aim of confirming the history of the mass transfer of TIC 308396022, we propose two plans for future works. The first is to perform detailed seismic modelling that includes the mass transfer from companions, since mass transfer may lead to incompatibility between the g- and p-mode pulsations and we are not able to find a normal single-star evolution model that fits both the g- and p-modes at the same time. The second is to conduct spectroscopic observations that may help to indicate an enhancement of s-process elements that are created during the AGB phase of the donor's evolution.

6. Conclusions

We analysed the pulsating behaviour of TIC 308396022 by using the three-year photometric observations delivered from the TESS mission, and extracted p- and g-mode pulsations from the 2-min cadence data with Fourier transform. The strongest peak $f_1 = 13.20362567(12)\,{\rm d}^{-1}$ is identified as the radial fundamental mode, and we also detected the first overtone at $f_2 = 17.003479(8)\,{\rm d}^{-1}$ and the second overtone at $f_3 = 21.052996(7)\,{\rm d}^{-1}$, which leads to the conclusion that this star is a new radial triple-mode HADS. Another strong mode at $f_4 = 18.96664(1)\,{\rm d}^{-1}$ is probably an $l = 1$ mode.

In the low-frequency region, we find an equally spaced period pattern with the period spacing $\Delta P = 2460$ s. The asymptotic spacing is measured as $\Pi_0 = 3655 \pm 13$ s, lower than most of the γ Dor stars in Li et al. (2019a). We propose that TIC 308396022 is the first radial triple-mode HADS with a g-mode period spacing pattern.

TIC 308396022 also shows clear orbital motion since its light maxima times and pulsation phases vary periodically. The orbit, which has a long period (803.5 ± 0.6 d), a very low eccentricity (0.015), and a small mass function, indicates that the system probably has undergone mass transfer and the companion is likely to be a C/O WD. Based on the derived luminosity $\log L/L_\odot = 0.97 \pm 0.02$, and the effective temperature $T_{\rm eff} = 7371 \pm 150$ K, TIC 308396022 lies near the bottom of the δ Sct instability strip. However, we were not able to find a theoretical model that matches the observed properties (L, $T_{\rm eff}$, f_1 and Π_0). Spectroscopic observations and detailed evolutionary–seismic modellings considering the mass accretion are needed to further reveal the history of this system.

Acknowledgements. This research is supported by the program of the National Natural Science Foundation of China (grant Nos. 11573021, U1938104 and 12003020). Gang Li acknowledges support from the project BEAMING ANR-18-CE31-0001 of the French National Research Agency (ANR) and from the Centre National d'Etudes Spatiales (CNES). We are grateful to the Australian Research Council for support (DP 210103119). This work has made use of data from the European Space Agency (ESA) mission *Gaia* (https://www.cosmos.esa.int/gaia), processed by the *Gaia* Data Processing and Analysis Consortium (DPAC, https://www.cosmos.esa.int/web/gaia/dpac/consortium). Funding for the DPAC has been provided by national institutions, in particular the institutions participating in the *Gaia* Multilateral Agreement. We would like to thank the TESS science team for providing such excellent data.

References

Aerts, C. 2021, Rev. Mod. Phys., 93, 015001
Aerts, C., Christensen-Dalsgaard, J., & Kurtz, D. W. 2010, Asteroseismology (Berlin: Springer)
Althaus, L. G., Córsico, A. H., Isern, J., et al. 2010, A&ARv, 18, 471
Antoci, V., Cunha, M., Houdek, G., et al. 2014, ApJ, 796, 118
Antoci, V., Cunha, M. S., Bowman, D. M., et al. 2019, MNRAS, 490, 4040
Baglin, A., Auvergne, M., Barge, P., et al. 2009, Transiting Planets, 253, 71
Bailer-Jones, C. A. L., Rybizki, J., Fouesneau, M., et al. 2021, AJ, 161, 147
Balona, L. A., Krisciunas, K., & Cousins, A. W. J. 1994, MNRAS, 270, 905
Balona, L. A., Lenz, P., Antoci, V., et al. 2012, MNRAS, 419, 3028
Bedding, T. R., Murphy, S. J., Colman, I. L., et al. 2015, Eur. Phys. J. Web Conf., 101, 01005
Bedding, T. R., Murphy, S. J., Hey, D. R., et al. 2020, Nature, 581, 147
Borucki, W. J., Koch, D., Basri, G., et al. 2010, Science, 327, 977
Bouabid, M.-P., Dupret, M.-A., Salmon, S., et al. 2013, MNRAS, 429, 2500
Bowman, D. M. 2017, Amplitude Modulation of Pulsation Modes in Delta Scuti Stars (Cham: Springer International Publishing)
Bowman, D. M., & Kurtz, D. W. 2018, MNRAS, 476, 3169
Bowman, D. M., Hermans, J., Daszyńska-Daszkiewicz, J., et al. 2021, MNRAS, 504, 4039
Bradley, P. A., Guzik, J. A., Miles, L. F., et al. 2015, AJ, 149, 68
Breger, M. 2000, ASP Conf. Ser., 210, 3
Breger, M., & Beichbuchner, F. 1996, A&A, 313, 851
Breger, M., Stich, J., Garrido, R., et al. 1993, A&A, 271, 482
Catelan, M., & Smith, H. A. 2015, Pulsating Stars (Weinheim: Wiley-VCH)
Chaplin, W. J., & Miglio, A. 2013, ARA&A, 51, 353
Christiansen, J. L., Derekas, A., Ashley, M. C. B., et al. 2007, MNRAS, 382, 239
Conroy, K. E., Prša, A., Stassun, K. G., et al. 2014, AJ, 147, 45
Córsico, A. H., Althaus, L. G., Miller Bertolami, M. M., et al. 2019, A&ARv, 27, 7
Deheuvels, S., Ballot, J., Gehan, C., et al. 2021, A&A, submitted [arXiv:2108.11848]
Dupret, M.-A., Grigahcène, A., Garrido, R., et al. 2004, A&A, 414, L17
Dupret, M.-A., Grigahcène, A., Garrido, R., et al. 2005a, MNRAS, 360, 1143
Dupret, M.-A., Grigahcène, A., Garrido, R., et al. 2005b, A&A, 435, 927
Fu, J. N., & Sterken, C. 2003, A&A, 405, 685
Gough, D. 2000, ASP Conf. Ser., 203, 529
Goupil, M.-J., Dupret, M. A., Samadi, R., et al. 2005, JApA, 26, 249
Grigahcène, A., Antoci, V., Balona, L., et al. 2010, ApJ, 713, L192
Guzik, J. A., Kaye, A. B., Bradley, P. A., et al. 2000, ApJ, 542, L57
Handler, G. 2009a, AIP Conf. Proc., 1170, 403
Handler, G. 2009b, MNRAS, 398, 1339
Handler, G. 2013, Planets, Stars and Stellar Systems. Volume 4: Stellar Structure and Evolution, 207
Handler, G., & Shobbrook, R. R. 2002, MNRAS, 333, 251
Hareter, M., Reegen, P., Miglio, A., et al. 2010, ArXiv e-prints [arXiv:1007.3176]
Henry, G. W., & Fekel, F. C. 2005, AJ, 129, 2026
Hey, D. R., Murphy, S. J., Foreman-Mackey, D., et al. 2020a, AJ, 159, 202
Hey, D., Murphy, S., Foreman-Mackey, D., et al. 2020b, J. Open Sour. Softw., 5, 2125
Holdsworth, D. L., Smalley, B., Gillon, M., et al. 2014, MNRAS, 439, 2078
Hurley, J. R., Pols, O. R., & Tout, C. A. 2000, MNRAS, 315, 543
Hurley, J. R., Tout, C. A., & Pols, O. R. 2002, MNRAS, 329, 897
Ivanova, N., Justham, S., Chen, X., et al. 2013, A&ARv, 21, 591

Karakas, A. I., Tout, C. A., & Lattanzio, J. C. 2000, MNRAS, 316, 689
Kaye, A. B., Handler, G., Krisciunas, K., Poretti, E., & Zerbi, F. M. 1999, PASP, 111, 840
Kjeldsen, H., & Bedding, T. R. 2012, IAU Symp., 285, 17
Kurtz, D. W., Saio, H., Takata, M., et al. 2014, MNRAS, 444, 102
Lauterborn, D. 1970, A&A, 7, 150
Lenz, P., & Breger, M. 2005, Commun. Asteroseismol., 146, 53
Li, G., Fu, J., Su, J., et al. 2018, MNRAS, 473, 398
Li, G., Van Reeth, T., Bedding, T. R., Murphy, S. J., & Antoci, V. 2019a, MNRAS, 487, 782
Li, G., Bedding, T. R., Murphy, S. J., et al. 2019b, MNRAS, 482, 1757
Li, G., Van Reeth, T., Bedding, T. R., et al. 2020, MNRAS, 491, 3586
Lomb, N. R. 1976, Ap&SS, 39, 447
McDonald, I., Zijlstra, A. A., & Watson, R. A. 2017, MNRAS, 471, 770
McNamara, D. H. 2000, in Delta Scuti and Related Stars, eds. M. Breger, & M. H. Montgomery, ASP Conf. Ser., 210, 373
Miglio, A., Montalbán, J., Noels, A., et al. 2008, MNRAS, 386, 1487
Miszuda, A., Szewczuk, W., & Daszyńska-Daszkiewicz, J. 2021, MNRAS, 505, 3206
Montgomery, M. H., & O'Donoghue, D. 1999, Delta Scuti Star Newsletter, 13, 28
Moravveji, E., Aerts, C., Pápics, P. I., et al. 2015, A&A, 580, A27
Murphy, S. J., & Shibahashi, H. 2015, MNRAS, 450, 4475
Murphy, S. J., Bedding, T. R., Shibahashi, H., et al. 2014, MNRAS, 441, 2515
Murphy, S. J., Shibahashi, H., & Bedding, T. R. 2016, MNRAS, 461, 4215
Murphy, S. J., Moe, M., Kurtz, D. W., et al. 2018, MNRAS, 474, 4322
Murphy, S. J., Hey, D., Van Reeth, T., et al. 2019, MNRAS, 485, 2380
Murphy, S. J., Saio, H., Takada-Hidai, M., et al. 2020, MNRAS, 498, 4272
Netzel, H., Pietrukowicz, P., Soszyński, I., et al. 2021, MNRAS, submitted [arXiv:2107.08064]
Ouazzani, R.-M., Salmon, S. J. A. J., Antoci, V., et al. 2017, MNRAS, 465, 2294
Ouazzani, R.-M., Lignières, F., Dupret, M.-A., et al. 2020, A&A, 640, A49
Paxton, B., Bildsten, L., Dotter, A., et al. 2011, ApJS, 192, 3
Paxton, B., Cantiello, M., Arras, P., et al. 2013, ApJS, 208, 4
Paxton, B., Marchant, P., Schwab, J., et al. 2015, ApJS, 220, 15
Paxton, B., Schwab, J., Bauer, E. B., et al. 2018, ApJS, 234, 34
Paxton, B., Smolec, R., Schwab, J., et al. 2019, ApJS, 243, 10
Peña, J. H., Villarreal, C., Piña, D. S., et al. 2016, Rev. Mex. Astron. Astrofis., 52, 385
Petersen, J. O. 1989, Delta Scuti Star Newsletter, 1, 6
Petersen, J. O., & Christensen-Dalsgaard, J. 1996, A&A, 312, 463
Poretti, E., Suárez, J. C., Niarchos, P. G., et al. 2005, A&A, 440, 1097
Poretti, E., Rainer, M., Weiss, W. W., et al. 2011, A&A, 528, A147
Ricker, G. R., Winn, J. N., Vanderspek, R., et al. 2014, Proc. SPIE, 9143, 914320
Ricker, G. R., Winn, J. N., Vanderspek, R., et al. 2015, J. Astron. Telesc. Instrum. Syst., 1, 014003
Rui, N. Z., & Fuller, J. 2021, MNRAS, 508, 1618
Sánchez Arias, J. P., Córsico, A. H., & Althaus, L. G. 2017, A&A, 597, A29
Saio, H., Kurtz, D. W., Takata, M., et al. 2015, MNRAS, 447, 3264
Saio, H., Takata, M., Lee, U., et al. 2021, MNRAS, 502, 5856
Scargle, J. D. 1982, ApJ, 263, 835
Schmid, V. S., & Aerts, C. 2016, A&A, 592, A116
Sekaran, S., Tkachenko, A., Johnston, C., et al. 2021, A&A, 648, A91
Shibahashi, H. 1979, PASJ, 31, 87
Shibahashi, H., & Kurtz, D. W. 2012, MNRAS, 422, 738
Shibahashi, H., Kurtz, D. W., & Murphy, S. J. 2015, MNRAS, 450, 3999
Stassun, K. G., Oelkers, R. J., Pepper, J., et al. 2018, AJ, 156, 102
Stellingwerf, R. F. 1979, ApJ, 227, 935
Sterken, C. 2005, ASP Conf. Ser., 335, 3
Tassoul, M. 1980, ApJS, 43, 469
Toonen, S., Voss, R., & Knigge, C. 2014, MNRAS, 441, 354
Townsend, R. H. D., & Teitler, S. A. 2013, MNRAS, 435, 3406
Ulusoy, C., Ulaş, B., Gülmez, T., et al. 2013, MNRAS, 433, 394
Uytterhoeven, K., Moya, A., Grigahcène, A., et al. 2011, A&A, 534, A125
Van Reeth, T., Tkachenko, A., Aerts, C., et al. 2015, ApJS, 218, 27
Van Reeth, T., Tkachenko, A., & Aerts, C. 2016, A&A, 593, A120
Wu, T., & Li, Y. 2019, ApJ, 881, 86
Wu, T., Li, Y., & Deng, Z.-M. 2018, ApJ, 867, 47
Wu, T., Li, Y., Deng, Z.-M., et al. 2020, ApJ, 899, 38
Xiong, D. R., Deng, L., Zhang, C., et al. 2016, MNRAS, 457, 3163
Yang, T. Z., & Esamdin, A. 2019, ApJ, 879, 59Y
Yang, T., Esamdin, A., Song, F., et al. 2018, ApJ, 863, 195
Ziaali, E., Bedding, T. R., Murphy, S. J., et al. 2019, MNRAS, 486, 4348
Zuo, Z. Y., & Li, X. D. 2014, MNRAS, 442, 1980